Valley-valve effect and even-odd chain parity in *p-n* graphene junctions

Alessandro Cresti,[1] Giuseppe Grosso,[1] and Giuseppe Pastori Parravicini[2]
[1]*NEST-CNR-INFM and Dipartimento di Fisica "E. Fermi," Università di Pisa, Largo Pontecorvo 3, I-56127 Pisa, Italy*
[2]*NEST-CNR-INFM and Dipartimento di Fisica "A. Volta," Università di Pavia, Via A. Bassi 6, I-27100 Pavia, Italy*
(Received 7 April 2008; published 11 June 2008)

We address the current blocking by a *p-n* junction in a zigzag graphene ribbon by means of numerical and analytic investigations. Ribbons with superimposed gate potentials perfectly block the current in the energy range, where a single energy band is active in both the *n* and the *p* regions, if the number of carbon chains is even. In the same conditions, an odd number of chains allows current transmission. We interpret this even-odd valley-valve effect in terms of the underlying honeycomb topology and crystal structure symmetry.

DOI: 10.1103/PhysRevB.77.233402 PACS number(s): 73.23.−b, 73.63.Nm

A few years ago, the experimental realization of graphene[1–3] has opened the path to countless investigations rich of developments and novelties[4–9] on a material of considerable theoretical and technological interest. The peculiar band structure of graphene makes possible the electrostatic control of carrier type, electronlike or holelike, and carrier density across the neutrality point. In graphene ribbons, local gates allow the fabrication of bipolar junctions,[10–14] as schematically shown in Fig. 1(a). The well-known two-valley band structure of the zigzag graphene ribbon is thus shifted in the region where the external potential is applied [Fig. 1(b)]. Consider carrier injection, e.g., from the right side of the junction at a positive energy E, where one single band is active on both sides of the ribbon [red dashed line in Fig. 1(b)]. The incoming current is supported by an electronlike state in the K valley [point A in Fig. 1(b)] and can propagate to the left, supported by a holelike state in the K' valley [point A' in Fig. 1(b)]. Transmission is thus possible only if the superimposed gate potential acts as an intervalley scattering source.[15–17] In the one-mode energy region, it has been observed[16] that transmission is allowed (forbidden) if the number of chains in the ribbon is odd (even). This striking valley-valve effect has been discussed in Refs. 15 and 16 and linked to the coupling of states localized at opposite edges of the ribbon.

In this Brief Report, we present numerical simulations of charge transport in a zigzag graphene ribbon, which evidence the even-odd effect and provide a theoretical interpretation based on general symmetry arguments on the bipartite honeycomb topology.

The dangling carbon orbitals on the honeycomb lattice give rise to bonding and antibonding π electronic states that cross the Fermi energy and play the key role in the transport properties.[4–6] For the numerical simulations, we adopt the orthogonal nearest-neighbor tight-binding Hamiltonian

$$H = E_0 \sum_i |\phi_i\rangle\langle\phi_i| + t \sum_{\langle ij \rangle} (|\phi_i\rangle\langle\phi_j| + |\phi_j\rangle\langle\phi_i|), \qquad (1)$$

where ϕ_i and ϕ_j denote the dangling p_z orbitals centered on the sites i and j of the lattice, $\langle ij \rangle$ denotes nearest-neighbor sites with hopping parameter $t \approx -3$ eV, and the orbital energy E_0 is taken as the reference energy (and set equal to zero). A superimposed potential is described by adding a term of the type

$$V = \sum_i V_i |\phi_i\rangle\langle\phi_i|, \qquad (2)$$

where V_i is the value of the potential on the site i. Within the above tight-binding model, we exploit the Keldysh formalism[18,19] to numerically evaluate the differential conductance for zigzag nanoribbons made up of $N_z=50$ and $N_z=51$ carbon chains. The efficient bond current formalism for the description and imaging of electron transport in graphene honeycomb lattices is reported in Refs 20 and 21. We consider the energy range $[-5\Delta, 5\Delta]$, where $\Delta = |t|\pi/(N_z+1/2)$ is the energy separation[21] between subsequent modes at the K point, see Fig. 1(b). Figure 2(a) shows the conductance for vanishing gate voltage. As expected, in the energy interval $[-(3/2)\Delta, (3/2)\Delta]$, the conductance is $2e^2/h$, while it assumes values $(2n+1)2e^2/h$ as successive conductive channels become active at higher energies.

We now consider the effect of a smooth potential step of the shape indicated in Fig. 2(b) and with height $V_g = \Delta, (3/2)\Delta, 2\Delta$. In the case $N_z=50$ and $V_g=\Delta$ [Fig. 2(c)], the junction is perfectly reflecting in the energy interval $0 < E < V_g = \Delta$. Furthermore, the conductance is unity in the energy intervals of width $(3/2)\Delta$ to the right of $E=\Delta$ and to

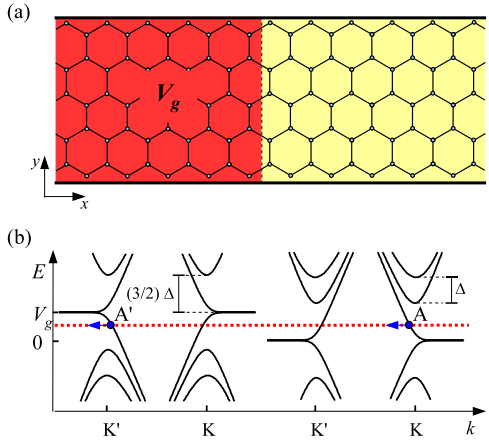

FIG. 1. (Color online) (a) Zigzag graphene nanoribbon with superimposed gate potential V_g. (b) Energy bands in the gated and neutral zones of the ribbon. Δ is the energy separation of the states at the Dirac points. The dashed red line indicates the energy of the injected electrons from the right side of the ribbon.

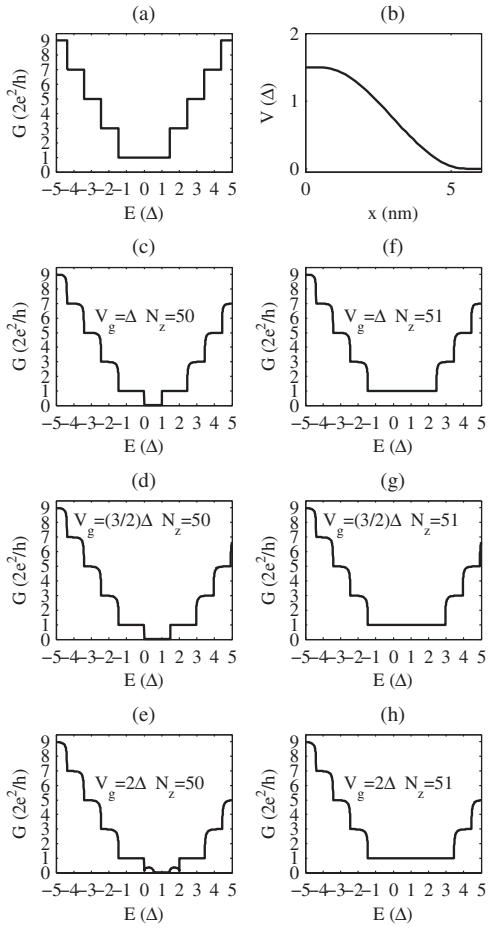

FIG. 2. (a) Conductance versus energy of the injected electrons for a graphene ribbon at $V_g=0$. (b) Spatial profile of the superimposed gate potential. (c), (d), and (e) Conductance for a ribbon with $N_z=50$ chains and superimposed potential $V_g=\Delta$, $(3/2)\Delta$, and 2Δ, respectively. (f), (g), and (h) Conductance for a ribbon with $N_z=51$ chains and superimposed potential $V_g=\Delta$, $(3/2)\Delta$, and 2Δ, respectively.

the left of $E=0$. Then, at successive energy increases in Δ, the conductance G approaches odd multiples of $2e^2/h$. In Fig. 2(d), the value of $V_g=(3/2)\Delta$ is considered, and the extension of the zero conductance region is maximal. With further increase in V_g, the region of zero conductance decreases [see Fig. 2(e) for $V_g=2\Delta$] and eventually disappears when $V_g>3\Delta$ because the multichannel regime is entered. For the same superimposed potential values, the situation is quite different for graphene ribbons with odd number of chains. The results are shown in Figs. 2(f)–2(h) in the case $N_z=51$. From the numerical results of Fig. 2, it is evident that in the energy regions of infinite resistance for N_z even, the current can flow for N_z odd.

In the following, we show that the above even-odd effect is deeply connected to the symmetry of the crystal structure and of the superimposed potential. To this aim, let us consider the unit cell of the structure of Fig. 3, containing $2N_z$ lattice points in the positions $\mathbf{d}_i$ $(i=1,2,\ldots,2N_z)$. From the $2N_z$ orbitals in the primitive cell, we build the $2N_z$ Bloch sums

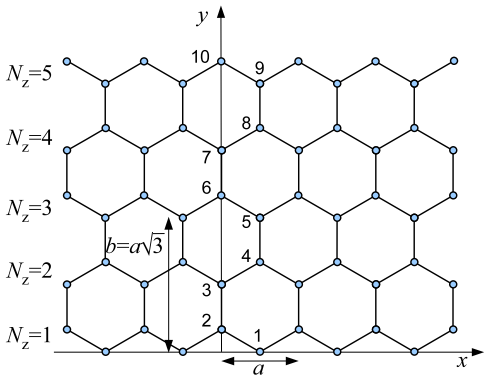

FIG. 3. (Color online) Structure of a graphene ribbon with $N_z=5$ zigzag chains and $2N_z$ carbon atoms in the primitive cell.

$$\Phi_i(k,\mathbf{r})=\frac{1}{\sqrt{N}}\sum_{\mathbf{t}_m} e^{i\mathbf{k}\cdot(\mathbf{t}_m+\mathbf{d}_i)}\phi_z(\mathbf{r}-\mathbf{t}_m-\mathbf{d}_i), \tag{3}$$

where $\mathbf{t}_m=(ma,0)$ are N lattice translation vectors, and $\mathbf{k}=(k,0)$ with k within the corresponding one-dimensional Brillouin zone, $-\pi/a<k\leq+\pi/a$. The crystalline wave functions can be expressed as linear combinations of Bloch sums

$$\Psi(k,\mathbf{r})=\sum_{i=1}^{2N_z} A_i(k)\Phi_i(k,\mathbf{r}). \tag{4}$$

On the basis set $\{\Phi_i\}$ $(i=1,2,\ldots,2N_z)$, the nearest-neighbor electronic Hamiltonian [Eq. (1)] is represented by a tridiagonal matrix of the type

$$H(k)=\begin{pmatrix} 0 & 2tc & 0 & 0 & \ldots \\ 2tc & 0 & t & 0 & \ldots \\ 0 & t & 0 & 2tc & \ldots \\ \ldots & \ldots & \ldots & \ldots & \ldots \end{pmatrix}_{2N_z}$$

$$\text{with} \quad c(k)=\cos(ka/2), \tag{5}$$

where the upper and lower diagonals have elements given alternately by $2t\cos(ka/2)$ and t. The Hamiltonian $H(k)$ can be represented by the finite chain model with $2N_z$ sites, as shown in Fig. 4.

The eigenvalues and eigenvectors of $H(k)$ give the energy

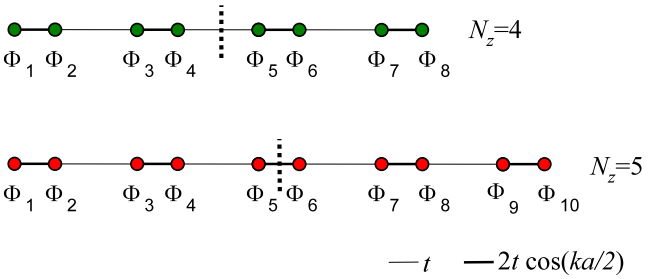

FIG. 4. (Color online) Schematic representation of Hamiltonian (5) for even N_z (with value $N_z=4$) and odd N_z (with $N_z=5$). The thin lines denote the off-diagonal matrix element t, while the thick lines denote the off-diagonal matrix element $2t\cos(ka/2)$.

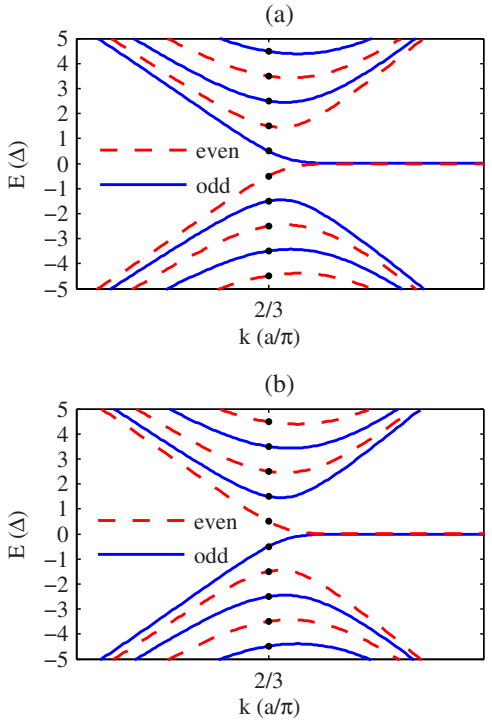

FIG. 5. (Color online) Band structure of a zigzag graphene ribbon composed of $N_z=50$ (a) and $N_z=51$ (b) chains. Solid black lines and dashed green lines indicate, respectively, odd and even parity of the corresponding wave functions. The energy unit Δ is the energy separation between adjacent bands at the Dirac point, as indicated by dots.

bands and the expansion coefficients of the crystalline wave functions for clean periodic ribbons. From the structure of the matrix $H(k)$ and its symmetry properties, which are evident from Fig. 4, it is seen that the eigenvectors are even or odd under mirror reflections with respect to the center of the finite chain. Thus the expansion coefficients $A_i(k)$ in Eq. (4) satisfy the relation

$$A_i = (-1)^p A_{2N_z+1-i} (i = 1,2, \ldots, 2N_z), \tag{6}$$

where the parity p is even or odd. Accordingly, the energy bands can be classified as even or odd. Although here we have only considered nearest-neighbor interactions, it should be noticed that the parity symmetry is preserved even in the case of higher order neighbor interactions, since it is controlled by the space mirror symmetry of the crystalline Hamiltonian.

The electronic structure and the parity of zigzag graphene ribbons with $N_z=50$ chains and $N_z=51$ chains are reported in Figs. 5(a) and 5(b), respectively. The flat parts of the bands near $E=0$ correspond to states localized at the edges for $k = \pm \pi/a$ and penetrating into the bulk as k approaches the Dirac points at $k= \pm 2\pi/3a$.[22,23]

We address now the possibility of intervalley-coupling by a superimposed potential on an otherwise clean and translationally invariant zigzag graphene ribbon. Since the gate potential is expressed as a diagonal perturbation on a given number of sites of the ribbon in real space, [see Eq. (2)], in order to evaluate the matrix elements of intervalley scattering among band states belonging to different valleys, it is convenient to introduce the site projection operators

$$P_{mj} = |\phi_z(\mathbf{r} - \mathbf{t}_m - \mathbf{d}_j)\rangle\langle\phi_z(\mathbf{r} - \mathbf{t}_m - \mathbf{d}_j)|, \tag{7}$$

which project the ribbon wave functions onto the jth site belonging to the unit cell specified by the mth translation vector. In particular, on the basis functions (3) we have the relation

$$\langle\Phi_i(k)|P_{mj}|\Phi_{i'}(q)\rangle = \frac{1}{N} e^{i(\mathbf{q}-\mathbf{k})\cdot(\mathbf{t}_m+\mathbf{d}_j)} \delta_{ij}\delta_{i'j}. \tag{8}$$

The gate potential (2) can be expressed as

$$V = \sum_{mj} V_{mj} P_{mj}, \tag{9}$$

where V_{mj} represents the superimposed potential on the indicated site. The matrix element of the perturbation potential between any two eigenfunctions $\Psi_a(k)$ and $\Psi_b(q)$ of the form (4) is

$$\langle\Psi_a(k)|V|\Psi_b(q)\rangle = \frac{1}{N}\sum_{mj} V_{mj} A_j^*(k) B_j(q) e^{i(\mathbf{q}-\mathbf{k})\cdot(\mathbf{t}_m+\mathbf{d}_j)}. \tag{10}$$

If we consider a gate potential that only varies along the longitudinal x direction and assumes the same values on all of the sites of a vertical column of the ribbon, we have in expression (10) $V_{mj}=V_m$. Then Eq. (10) can be recast in the form

$$\langle\Psi_a(k)|V|\Psi_b(q)\rangle = S\frac{1}{N}\sum_{m} V_m e^{i(\mathbf{q}-\mathbf{k})\cdot\mathbf{t}_m}, \tag{11}$$

where the structurelike factor S is given by

$$S = \sum_{j=1}^{2N_z} A_j^*(k) B_j(q) e^{i(\mathbf{q}-\mathbf{k})\cdot\mathbf{d}_j}. \tag{12}$$

Notice that the sum in S only involves the sites of the primitive cell and the expansion coefficients $A_i(k)$ and $B_j(q)$ of the wave functions $\Psi_a(k)$ and $\Psi_b(q)$, respectively. The structure factor is different for even or odd ribbons, and this is at the origin of the observed even-odd effect in charge transport. In fact, by exploiting Eq. (6), expression (12) can be recast in the form

$$S = \sum_{j=1}^{N_z} A_j^*(k) B_j(q) (e^{i(\mathbf{q}-\mathbf{k})\cdot\mathbf{d}_j} + (-1)^{p_a+p_b} e^{i(\mathbf{q}-\mathbf{k})\cdot\mathbf{d}_{2N_z+1-j}}), \tag{13}$$

where p_a and p_b are the parities of the wave functions Ψ_a and Ψ_b, respectively.

We apply now the above relation to the case that one wave function is even and the other is odd; in this case, in expression (13) it holds $(-1)^{p_a+p_b}=-1$. If the number N_z of zigzag chains is even, we have that the x components of the vectors $\mathbf{d}_j$ and $\mathbf{d}_{2N_z+1-j}$ are equal (see Fig. 3), thus, each term in the parenthesis of Eq. (13) vanishes. This does not hold in

the case of odd number of chains. These results entail perfect reflection in the case of a ribbon with even number of chains, while transmission is possible for an odd number of chains. In the case Ψ_a and Ψ_b have the same parity, $(-1)^{p_a+p_b}=1$ and in general $S\neq 0$ independently of the number of chains N_z.

The above considerations demonstrate that the parity of the number of chains of the ribbon in stepwise superimposed gate potentials are responsible for the observed even-odd effect in charge transport in *p-n* junctions when a single transmission mode is active throughout the whole ribbon. The field-effect blocking of currents in the analyzed geometrical arrangement and energy range in graphene nanoribbons opens applicative perspectives[15,16] for quantum logic gates besides the more traditional ones based on semiconductor quantum wires[24,25] and electronic spin manipulation.[26] The numerical results and the analytic interpretation presented in this Brief Report can be extended to other graphene architectures and other materials[27] with honeycomb lattice structure, in view of a deeper understanding and better control of the valley degrees of freedom in this class of two-dimensional electronic devices.

This work has been supported by Scuola Normale Superiore, and by National Enterprise for Nanoscience and Nanotechnology (NEST).

[1] K. S. Novoselov, A. K. Geim, S. V. Morozov, D. Jiang, Y. Zhang, S. V. Dubonos, I. V. Grigorieva, and A. A. Firsov, Science **306**, 666 (2004).
[2] K. S. Novoselov, A. K. Geim, S. V. Morozov, D. Jiang, M. I. Katsnelson, I. V. Grigorieva, S. V. Dubonos, and A. A. Firsov, Nature (London) **438**, 197 (2005).
[3] Y. Zhang, Y.-W. Tan, H. L. Stormer, and P. Kim, Nature (London) **438**, 201 (2005).
[4] R. Saito, G. Dresselhaus, and M. S. Dresselhaus, *Physical Properties of Carbon Nanotubes* (Imperial College Press, London, 1998).
[5] J.-C. Charlier, X. Blase, and S. Roche, Rev. Mod. Phys. **79**, 677 (2007).
[6] N. M. R. Peres, F. Guinea, and A. H. Castro Neto, Phys. Rev. B **73**, 125411 (2006).
[7] T. Stauber and N. M. R. Peres, J. Phys.: Condens. Matter **20**, 055002 (2008).
[8] C. Berger, Z. Song, X. Li, X. Wu, N. Brown, C. Naud, D. Mayou, T. Li, J. Hass, A. N. Marchenkov, E. H. Conrad, P. N. First, and W. A. de Heer, Science **312**, 1191 (2006).
[9] B. Partoens and F. M. Peeters, Phys. Rev. B **74**, 075404 (2006); **75**, 193402 (2007).
[10] J. R. Williams, L. DiCarlo, and C. M. Marcus, Science **317**, 638 (2007).
[11] D. A. Abanin and L. S. Levitov, Science **317**, 641 (2007).
[12] B. Huard, J. A. Sulpizio, N. Stander, K. Todd, B. Yang, and D. Goldhaber-Gordon, Phys. Rev. Lett. **98**, 236803 (2007).
[13] B. Özyilmaz, P. Jarillo-Herrero, D. Efetov, D. A. Abanin, L. S. Levitov, and P. Kim, Phys. Rev. Lett. **99**, 166804 (2007).
[14] F. Molitor, J. Güttinger, C. Stampfer, D. Graf, T. Ihn, and K. Ensslin, Phys. Rev. B **76**, 245426 (2007).
[15] A. Rycerz, J. Tworzydło, and C. W. J. Beenakker, Nat. Phys. **3**, 172 (2007).
[16] A. R. Akhmerov, J. H. Bardarson, A. Rycerz, and C. W. J. Beenakker, Phys. Rev. B **77**, 205416 (2008).
[17] K. Wakabayashi and T. Aoki, Int. J. Mod. Phys. B **16**, 4897 (2002).
[18] D. K. Ferry and S. M. Goodnick, *Transport in Nanostructures* (Cambridge University Press, Cambridge, 1997).
[19] R. Lake, G. Klimeck, R. C. Bowen, and D. Jovanovic, J. Appl. Phys. **81**, 7845 (1997).
[20] L. P. Zârbo and B. K. Nikolić, Europhys. Lett. **80**, 47001 (2007).
[21] A. Cresti, G. Grosso, and G. Pastori Parravicini, Phys. Rev. B **76**, 205433 (2007); **77**, 115408 (2008).
[22] M. Fujita, K. Wakabayashi, K. Nakada, and K. Kusakabe, J. Phys. Soc. Jpn. **65**, 1920 (1996).
[23] K. Nakada, M. Fujita, G. Dresselhaus, and M. S. Dresselhaus, Phys. Rev. B **54**, 17954 (1996).
[24] R. W. Keyes, J. Phys.: Condens. Matter **18**, S703 (2006).
[25] T. Zibold, P. Vogl, and A. Bertoni, Phys. Rev. B **76**, 195301 (2007).
[26] G. Burkard, J. Phys.: Condens. Matter **19**, 233202 (2007).
[27] K. S. Novoselov, D. Jiang, F. Schedin, T. J. Booth, V. V. Khotkevich, S. V. Morozov, and A. K. Geim, Proc. Natl. Acad. Sci. U.S.A. **102**, 10451 (2005).